J. Phys. Chem. B 1997, 101, 3727−3733

Cesium-133 NMR Study of $CsCd(SCN)_3$: Relative Orientation of the Chemical Shift and Electric Field Gradient Tensors

Scott Kroeker,[†] Klaus Eichele,[†] Roderick E. Wasylishen,[†,*] and James F. Britten[‡]

Department of Chemistry, Dalhousie University, Halifax, Nova Scotia, Canada B3H 4J3, and
Department of Chemistry, McMaster University, Hamilton, Ontario, Canada L8S 4M1

Received: December 19, 1996[⊗]

Single-crystal NMR was used to characterize the cesium-133 chemical shift and electric field gradient (EFG) tensors in $CsCd(SCN)_3$. The principal axes of the two interaction tensors are not coincident, a reflection of the general positioning of cesium nuclei within the unit cell. Relative orientations of the chemical shift and EFG tensors have been determined, but assignment of the two magnetically distinct sites remains elusive. The span of the chemical shift, 94.4 ppm, is moderate in comparison with other cesium salts, and the magnitude of the nuclear quadrupole coupling constant, 148 kHz, is in the midrange of those reported for cesium compounds. Excellent agreement is observed between experimental ^{133}Cs NMR spectra of a stationary powder sample and spectra calculated using NMR parameters from the single-crystal analysis. Moreover, simulations indicate that the static line shape is very sensitive to the relative orientation of the chemical shift and EFG tensors. Experimental ^{133}Cs NMR spectra obtained with magic-angle and variable-angle spinning are well reproduced by calculations utilizing single-crystal NMR data.

Introduction

Of the quadrupolar nuclei, cesium-133 is unusually favorable for study by NMR. Its 100% natural abundance combines with a relatively large magnetic moment to produce a receptivity 270 times that of ^{13}C at a constant field.[1,2] A spin $^7/_2$ nucleus, ^{133}Cs has a moderate chemical shift range of about 600 ppm—the largest of the alkali-metal nuclei. Moreover, in the applied magnetic fields of typical NMR experiments, the nuclear quadrupole interaction is sufficiently small that first-order perturbation theory is usually adequate to describe the resulting line shape.

Cesium is found in many important materials, and solid-state cesium-133 NMR has played a crucial role in their study. Applications of ^{133}Cs NMR to such a variety of materials as clay minerals,[3,4] zeolites,[5−8] semiconductors,[9] alkalides and electrides,[10] and doped fullerene superconductors[11−13] have provoked interest in a more complete understanding of the fundamental interactions underlying the observed spectra.

Until recently, the assumption that the chemical shielding and electric field gradient (EFG) tensors are coincident was prevalent in the analysis of NMR spectra of quadrupolar nuclei. In fact, prior to 1990, there were only two reports of noncoincidence of these tensors.[14,15c] This assumption may have stemmed from the practical difficulties associated with theoretical treatments of spin systems involving both interactions in a general orientation with respect to one another. In particular, analytical expressions can be developed if the tensor orientations are assumed coincident;[16] otherwise, numerical simulations are required. Moreover, many of the early investigations were performed using electromagnets where low fields rendered the chemical shielding interaction negligible, thus tacitly sustaining the assumption.

Two factors can be identified in the dismantling of this assumption. First, from a pragmatic perspective, the development of faster computers has facilitated the calculation of spectra using numerical simulations. Efficiency was further improved with the introduction of the powder-averaging algorithm by Alderman et al.[17] Taken together, computations that were essentially intractable in the 1970s became trivial in the 1990s. Second, the growing number of examples of tensor noncoincidence has begun to demonstrate that coincidence of the chemical shielding and electric field gradient tensors, when not required by symmetry, is merely a coincidence. From a theoretical perspective, this assertion comes as no surprise, since the physical origin of these interactions is completely different: the electric field gradient is a first-order property, whereas chemical shielding is a second-order property.[18]

A variety of methods has been employed in determining the relative orientation of these nuclear interactions. Single-crystal NMR has played a crucial role in this regard,[14,15,19−22] primarily because of the straightforward, if somewhat tedious, analysis of the data to yield unambiguous tensor orientations with respect to the crystal frame.[23] Gornostansky and Stager's 1967 ^{51}V NMR study[14] of a single crystal of vanadium pentoxide represents the first example in which the EFG and chemical shielding tensors were found to be noncoincident. Other investigations of these tensors by single-crystal NMR have focused on ^{59}Co in $K_3Co(CN)_6$ and $Co(acetylacetonate)_3$,[15] ^{17}O in benzophenone,[19] ^{133}Cs in Cs_2HgBr_4,[20] Cs_2SO_4,[24] and Cs_2CrO_4,[21] and ^{87}Rb in Rb_2CrO_4,[25] $RbClO_4$, and Rb_2SO_4.[22]

Considerable effort has been devoted to the development of techniques for extracting chemical shift and EFG tensors from NMR spectra of powder samples.[26−36] Several magic-angle spinning (MAS)[32,33] and variable-angle spinning (VAS)[35,36] experiments, for example, have been used. In some cases, these methods yield reliable EFG and chemical shift parameters; however, it is more difficult to obtain information about the relative orientation of these tensors. Regardless of the confidence one places in the *relative* tensor orientations, powder NMR methods can offer no insight about the *absolute* orientations of the tensors with respect to the crystal axes, in the absence of special symmetry.

In this paper, we report a cesium-133 single-crystal NMR study of $CsCd(SCN)_3$. The crystal structure indicates that cesium nuclei lie in general positions and no symmetry restrictions are incumbent upon the tensor orientations. Also presented are ^{133}Cs NMR spectra of spinning and stationary powder samples of $CsCd(SCN)_3$. Successful simulations of

---

[*] Author to whom correspondence should be addressed. Phone: 902-494-2564. Fax: 902-494-1310. E-mail: rodw@is.dal.ca.

[†] Dalhousie University.

[‡] McMaster University.

[⊗] Abstract published in *Advance ACS Abstracts,* April 15, 1997.

S1089-5647(97)00043-6 CCC: $14.00

spectra using data obtained from the single-crystal analysis confirm the single-crystal results.

Experimental Section

Materials. Cesium trithiocyanatocadmate, $CsCd(SCN)_3$, was prepared by dissolving stoichiometric amounts of $Cd(SCN)_2$ and CsSCN in a 1:2 ethanol–water mixture.[37] Slow evaporation of the solvent yielded large crystals of the title compound. Cadmium thiocyanate was prepared by metathesis of cadmium sulfate and barium thiocyanate.[38] Cesium thiocyanate was synthesized in a similar fashion, from cesium carbonate and ammonium thiocyanate in water. Starting materials were obtained from commercial sources and used without further purification.

Single-Crystal NMR. A crystal of $CsCd(SCN)_3$ was mounted in a hollow, three-sided, 4-mm^3 alumina cube. The orientation of the crystal axes with respect to the cube frame was determined by placing the mounted crystal on an X-ray diffractometer and indexing a sufficient number of reflections. Cesium-133 NMR spectra of the crystal were acquired at 52.48 MHz on a Bruker AMX-400 spectrometer (9.4 T) with a Doty single-crystal probe (Doty Scientific, Columbia, SC). The sweep width was 200 kHz, and 64 transients were coadded. Each spectrum consisted of 2 K points zero-filled to 4 K. The "solution $\pi/2$" pulse width was calibrated using a solution of 0.5 M CsCl(aq) to be 2.5 μs ($\nu_{rf} = 100$ kHz). For the crystal, a small flip angle corresponding to about 30° was used. Due to the long ^{133}Cs nuclear spin–lattice relaxation time, a recycle delay of 2 min was required. Spectra were referenced to the 0.5 M CsCl(aq) peak.

NMR Spectra of Powders. A static spectrum of $CsCd(SCN)_3$ at 52.48 MHz was obtained using a 5-mm Bruker probe with a solenoidal coil oriented perpendicular to the applied magnetic field. A finely ground sample was packed into about 1 cm of a 5-mm-diameter glass NMR tube and plugged. This tube was placed in the center of the coil. The solution $\pi/2$ pulse width was 2.9 μs ($\nu_{rf} = 86$ kHz). One quarter of this value was used for the single-pulse excitation. A spectral width of 100 kHz was used. Eight hundred eighty scans were collected with a recycle delay of 2 min. Each transient consisted of 2 K points zero-filled to 4 K.

MAS and VAS NMR spectra were obtained at 26.24 MHz using a Bruker MSL-200 spectrometer operating at 4.7 T. Rotors (7 mm) were packed with a finely ground sample and spun at 3–4 kHz. A typical experiment utilized a 125-kHz spectral width, coadding several hundred transients of 8 K data points. Before Fourier transformation, the data file was zero-filled to 16 K. A recycle delay of 2 min was used, and ν_{rf} ranged from 40 kHz for the MAS spectrum to 67 kHz for the VAS spectra. VAS experiments were carried out with a Bruker MAS probe by changing the angle of rotation from 54.74°. Calibration of the spinning angle utilized the central transition of CsSCN *(vide infra).*

Spectral Simulations. NMR spectral simulations of stationary and spinning samples were performed using QUADSPIN, a C program developed in this lab which utilizes the powder-averaging algorithm of Alderman et al.[17] For spinning samples, QUADSPIN computes the free induction decay of a spin system subject to both chemical shielding and a first-order quadrupole perturbation. This program accounts for a general relative orientation of these tensors and, in spinning powder simulations, a general axis of rotation with respect to the applied magnetic field direction. These calculations were carried out with an IBM 80486 and a SGI Indy workstation equipped with a R4600 processor.

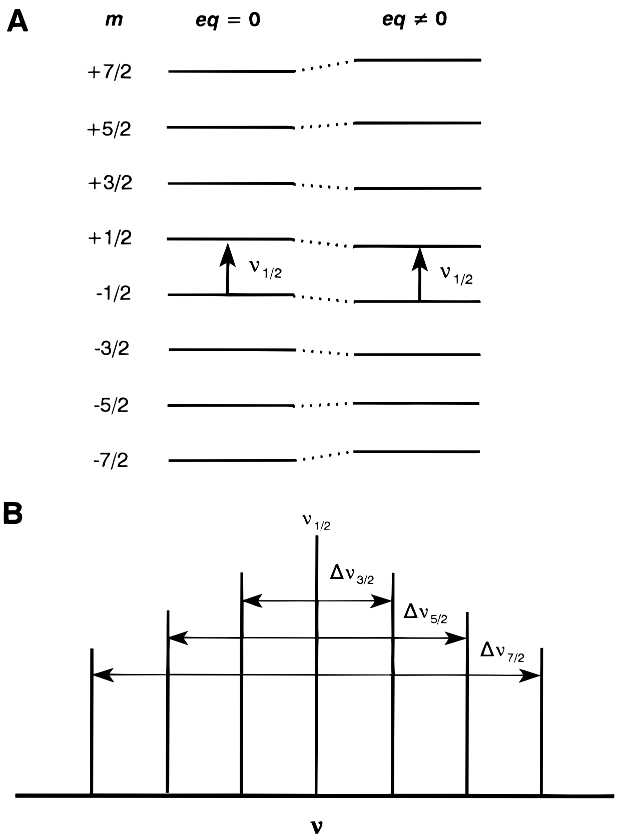

Figure 1. (A) Energy levels of a spin $^7/_2$ nucleus for a particular crystallite orientation in an applied magnetic field and (B) the resulting NMR spectrum.

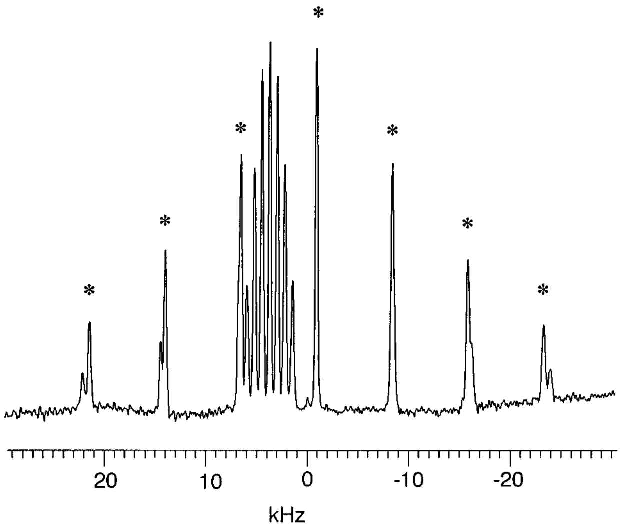

Figure 2. Typical cesium-133 NMR spectrum of a $CsCd(SCN)_3$ crystal. All peaks arising from one of the magnetically distinct sites are indicated by asterisks. Shoulders visible near the outermost sets of satellites are due to crystal twinning.

Results and Discussion

Single-Crystal NMR Spectra. The energy level diagram of a spin $^7/_2$ nucleus in a strong magnetic field consists of eight energy levels and, hence, seven single-quantum transitions (Figure 1). A typical ^{133}Cs NMR spectrum of the $CsCd(SCN)_3$ single crystal is shown in Figure 2. From this spectrum, it is evident that two seven-peak patterns are present. In order to understand this, one must examine the space group symmetry of the crystal.

$CsCd(SCN)_3$ crystallizes in a monoclinic lattice, with the space group $P2_1/c$.[37] Four formula units are present in the unit

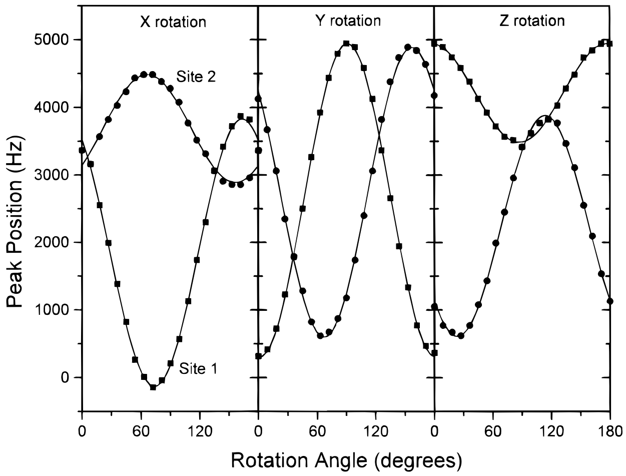

Figure 3. Rotation plots illustrating variations in the cesium-133 central transition peak position as a function of the rotation angle. Solid lines represent fits to eq 1.

cell, but all cesium nuclei are crystallographically equivalent. Crystallographic equivalence arises from nuclei which are related by any symmetry operation and demands only that the principal components of the interaction tensors be identical. Thus, in a powder sample, a single site is observed in the ^{133}Cs NMR spectrum *(vide infra)*. However, in order to predict how many signals will be observed in the single-crystal NMR spectrum, it is necessary to consider the distinction between *crystallographic* and *magnetic* equivalence. Magnetic equivalence emerges when nuclei are related by symmetry elements that retain an equivalent orientation with respect to the applied magnetic field. Sites related by a center of inversion, for instance, are magnetically equivalent, whereas rotation axes or mirror planes imply magnetic nonequivalence. Clearly, it is possible for multiple signals to be observed from a crystal with a single crystallographic site if they are symmetry-related in such a way that their principal components are not oriented identically. In the case of CsCd(SCN)$_3$, a given cesium nucleus in the unit cell is related to another in the cell by an inversion center (magnetically equivalent) and the remaining two by a screw axis (magnetically nonequivalent). Consequently, the resulting spectrum consists of two seven-peak patterns reflecting this symmetry arrangement. Due to the crystallographic equivalence, the principal components of the chemical shielding and nuclear quadrupole interaction tensors obtained from analysis of each magnetically distinct site will be identical, but their orientations will be related by rotation about the crystal *b* axis.

Cesium-133 NMR spectra were acquired as a function of crystal orientation in the magnetic field. Rotations were performed about the orthogonal *X*, *Y*, and *Z* axes of the cube frame, with 21 spectra acquired for each rotation; these corresponding to 9° increments of the rotation angle, ψ. Each peak was assigned to the appropriate transition and site. Observed central transition positions were fit to sinusoidal curves to obtain parameters related to the chemical shift tensor (Figure 3):[23]

$$\nu_i^\sigma(\psi) = A_i^\sigma + B_i^\sigma \cos 2\psi + C_i^\sigma \sin 2\psi \qquad (i = X, Y, Z) \quad (1)$$

since the central transition is unaffected to first order by the quadrupole interaction. A set of coefficients, A^σ, B^σ, and C^σ, was generated for each rotation, yielding nine for each site (Table 1). These are related to the chemical shift tensor in the cube frame according to the following expressions:

TABLE 1: Cesium-133 Chemical Shift Parameters, in Hz,[a] from a Least-Squares Fit of Central Transition Peak Positions in CsCd(SCN)$_3$ at 52.48 MHz. Standard Deviations Given in Parentheses

parameter	site 1	site 2
A_X^σ	1860(20)	3690(20)
B_X^σ	1660(20)	−540(30)
C_X^σ	−1080(20)	580(30)
A_Y^σ	2628(8)	2750(10)
B_Y^σ	−2320(10)	1490(20)
C_Y^σ	−80(10)	−1540(20)
A_Z^σ	4220(8)	2250(10)
B_Z^σ	720(10)	−1120(10)
C_Z^σ	−80(10)	−1190(20)

[a] Referenced to 0.5 M CsCl(aq) at 0.0 Hz.

TABLE 2: Averaged Cesium-133 Chemical Shift Tensor Principal Components in ppm[a] (Top Row) and Direction Cosines Relative to the Orthogonalized Crystal Frame (Bottom Rows) in CsCd(SCN)$_3$[b]

δ_{11}	δ_{22}	δ_{33}
93.8[c]	72.6[c]	−0.6[c]
−0.822	−0.367	−0.435
+0.544	−0.283	−0.790
+0.167	−0.886	+0.433

[a] Referenced to 0.5 M CsCl(aq) at 0.0 ppm. [b] Direction cosines of site 2 can be generated from those of site 1 by ($\bar{x}$, y, $\bar{z}$). [c] Errors in the principal components estimated to be ±0.5 ppm.

$$\nu_{XX}^\sigma = \frac{1}{2}(A_Y^\sigma - B_Y^\sigma + A_Z^\sigma + B_Z^\sigma) \quad (2)$$

$$\nu_{YY}^\sigma = \frac{1}{2}(A_Z^\sigma - B_Z^\sigma + A_X^\sigma + B_X^\sigma) \quad (3)$$

$$\nu_{ZZ}^\sigma = \frac{1}{2}(A_X^\sigma - B_X^\sigma + A_Y^\sigma + B_Y^\sigma) \quad (4)$$

$$\nu_{XY}^\sigma = \nu_{YX}^\sigma = -C_Z^\sigma \quad (5)$$

$$\nu_{XZ}^\sigma = \nu_{ZX}^\sigma = -C_Y^\sigma \quad (6)$$

$$\nu_{YZ}^\sigma = \nu_{ZY}^\sigma = -C_X^\sigma \quad (7)$$

Upon diagonalization of the chemical shift tensor, one obtains the principal values, $\nu_{11}{}^\sigma$, $\nu_{22}{}^\sigma$, $\nu_{33}{}^\sigma$ and the direction cosines relating the principal axis system (PAS) of the chemical shift tensor to the cube frame. The chemical shift tensor averaged from the two sites has a span of 94.4(5) ppm and an isotropic value of 55.3(5) ppm; the asymmetry in the chemical shift tensor, η_{CS}, is 0.38(5). The Euler angles rotating the cube frame into the orthogonalized crystal frame, *(a*, b, c)*, are $\alpha' = 98.7°$, $\beta' = 98.4°$, and $\gamma' = 240.3°$. By rotation according to these angles, the orientation of each chemical shift PAS in the crystal frame was determined (Table 2).

A similar procedure was followed in the analysis of the quadrupole-induced splittings. Since the observed splittings, $\Delta\nu_m = \nu_{m\leftrightarrow m-1} - \nu_{1-m\leftrightarrow -m}$, between symmetrical satellite peaks are related to the nuclear quadrupole interaction in the laboratory frame by a constant, one approach is to average the satellite splittings:[21]

$$\frac{eQV_{zz}}{h} = \frac{7}{18}[6\Delta\nu_{3/2} + 3\Delta\nu_{5/2} + 2\Delta\nu_{7/2}] \quad (8)$$

where z is the direction of the applied magnetic field and V_{zz} represents the z component of the electric field gradient, eq_{zz}.

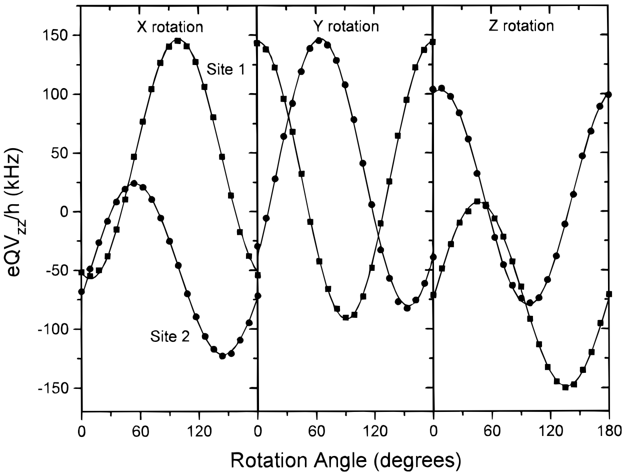

Figure 4. Rotation plots illustrating variations in the cesium-133 quadrupolar interaction in the laboratory frame (eq 8) as a function of the rotation angle. Solid lines represent fits to eq 9.

TABLE 3: Cesium-133 Quadrupole Splitting Parameters for CsCd(SCN)$_3$, in kHz, from a Least-Squares Fit to Equation 9. Standard Deviations Given in Parentheses

parameter	site 1	site 2
A_X^Q	45.0(5)	−48.5(2)
B_X^Q	−96.6(5)	−23.8(5)
C_X^Q	−32.0(5)	68.8(5)
A_Y^Q	26.8(5)	33.4(7)
B_Y^Q	118.1(7)	−71.4(9)
C_Y^Q	2.1(3)	88.4(9)
A_Z^Q	−70.2(2)	12.1(5)
B_Z^Q	−3.0(5)	88.4(5)
C_Z^Q	78.2(5)	23.1(5)

This averaged value was plotted as a function of ψ for each rotation (Figure 4) and fit to

$$\frac{eQV_{zz}(\psi)_i}{h} = A_i^Q + B_i^Q \cos 2\psi + C_i^Q \sin 2\psi \quad (i = X, Y, Z) \tag{9}$$

thereby yielding a set of nine coefficients for each site (Table 3). These are related to the nuclear quadrupole interaction tensor, eQV_{ij}/h, in the cube frame according to the following expressions:[39]

$$\frac{eQV_{XX}}{h} = \frac{1}{3}(-2A_X^Q + A_Y^Q - B_Y^Q + A_Z^Q + B_Z^Q) \tag{10}$$

$$\frac{eQV_{YY}}{h} = \frac{1}{3}(-2A_Y^Q + A_Z^Q - B_Z^Q + A_X^Q + B_X^Q) \tag{11}$$

$$\frac{eQV_{ZZ}}{h} = \frac{1}{3}(-2A_Z^Q + A_X^Q - B_X^Q + A_Y^Q + B_Y^Q) \tag{12}$$

$$\frac{eQV_{XY}}{h} = \frac{eQV_{YX}}{h} = -C_Z^Q \tag{13}$$

$$\frac{eQV_{XZ}}{h} = \frac{eQV_{ZX}}{h} = -C_Y^Q \tag{14}$$

$$\frac{eQV_{YZ}}{h} = \frac{eQV_{ZY}}{h} = -C_X^Q \tag{15}$$

TABLE 4: Averaged ^{133}Cs Nuclear Quadrupole Interaction Tensor Principal Components, in kHz (Top Row), and Direction Cosines Relative to the Orthogonalized Crystal Frame (Bottom Rows) of CsCd(SCN)$_3$[a]

eQV_{11}/h	eQV_{22}/h	eQV_{33}/h
1.17[b]	147.2[b]	−148.4[b]
+0.480	−0.490	−0.727
−0.249	−0.871	+0.423
−0.841	−0.022	−0.540

[a] Direction cosines of site 2 can be generated from those of site 1 by $(\bar{x}, y, \bar{z})$. [b] Errors in the principal components estimated to be ±3 kHz.

Diagonalization of the eQV_{ij}/h tensor yields principal components eQV_{11}/h, eQV_{22}/h, and eQV_{33}/h. The direction cosines orienting these components in the cube frame can be rotated into the crystal frame, as for the chemical shift tensor (Table 4). The magnitude of the quadrupole coupling constant is the largest component, $eQV_{33}/h = 148(3)$ kHz. Utilizing the following convention for the EFG tensor principal components,

$$|V_{33}| \geq |V_{22}| \geq |V_{11}| \tag{16}$$

one can also obtain the asymmetry in the quadrupole interaction tensor,

$$\eta_Q = \frac{V_{11} - V_{22}}{V_{33}} = 0.98(3) \tag{17}$$

From the direction cosines, it is clear that the chemical shift and EFG tensors are not coincident. The Euler angles relating the chemical shift PAS to the EFG have been derived according to the convention that α represents a positive rotation about the z axis of the EFG tensor in its PAS, β represents a positive rotation about the new y axis, and γ is a positive rotation about the new z axis. Thus, $\alpha = 113°$, $\beta = 105°$, and $\gamma = 140°$.

One can make use of the symmetry relationship between the two magnetically distinct sites to arrive at an estimate of the errors to which these results are subject. First, since the nuclei are crystallographically equivalent, the principal components for the two sites should be equal. Hence, the difference in these is indicative of the minimum error associated with the magnitudes. Second, according to the crystal symmetry, rotation of one experimentally determined tensor by 180° about the crystallographic b axis should align the principal axes. To the extent that these axes differ, one has a measure of the error associated with the absolute orientations. On this premise, we find the absolute orientations to be accurate to about 3°.

Assignment of Tensor Orientations. The presence of two magnetically inequivalent cesium sites raises the question of assignment: which set of tensor orientations corresponds to which cesium site in the unit cell? A variety of approaches has been considered to distinguish between the two possible assignments.

To assign the orientation of the chemical shift tensors, one might attempt to calculate the chemical shielding of a cesium nucleus in the unit cell. Although *ab initio* calculations of chemical shieldings are becoming increasingly reliable for first- and second-row elements, trustworthy computations of heavier elements such as cesium are not yet feasible.[40,41] Moreover, the covalent nature of the bonding in many of the well-studied elements permits calculations to be performed on a single molecule. For an ionic system like the one at hand, it would be necessary to include some reasonably sized volume surrounding the atoms of interest. While this may be possible for systems with fewer, or lighter, ions, the constituent components of the unit cell of interest would require prohibitively lengthy computational times to obtain meaningful results at the present time.

Chemical shift tensor assignments may be based on qualitative considerations of the local cesium environments. In some cases, for example, the nuclei of interest occupy special positions in the cell which place symmetry constraints on the orientations. This is not so in $CsCd(SCN)_3$—cesium placements are completely general. For some nuclei, empirical guidelines have been offered for understanding their orientations. From a close examination of the local environment at the two magnetically nonequivalent sites, it is impossible to assign the sites based on their chemical shifts. Cesium nuclei are relatively isolated with respect to the $[Cd(SCN)_3]^-$ network. It is necessary to conclude that any relationship between the local structure and the orientation of the ^{133}Cs chemical shielding tensor is governed by subtle and complicated effects which are not apparent upon inspection.

A similar approach can, in principle, be employed to adjudicate between the orientations of the EFG tensors. In this case, however, qualitative arguments based on local symmetry and structural characteristics are even less trustworthy, since the EFG tensor is known to be sensitive to longer range effects than the chemical shielding tensor. More promising is the point charge model described by Slichter.[42] This model has been used extensively over the years and has proven itself to be a reliable tool when care is taken in interpreting the results.[21,32d] In essence, this model simply considers each atom in the lattice as a point charge and computes the electric field gradient at a particular position. In its application to this system, the computed EFG tensor for a given cesium nucleus reproduces the relative magnitudes of the principal components adequately. The result of greatest interest, however, is the orientation of these components, and this is found to compare equally well to either experimental orientation. For example, the largest component determined by the point charge model essentially bisects the angle formed between the largest components of the two sites.

The failure of the point charge model to aid in the assignment of the two orientations merits a few comments. At first, the special utility of this method for ionic systems appears to be an advantage for the case of $CsCd(SCN)_3$. A problem is encountered, however, in assigning charges to the thiocyanate anion. Clearly, it cannot be treated as a point charge, but the distribution of charge among the three constituent atoms is not obvious. Based on the natural bond orbital charges from a high-level *ab initio* calculation of the SCN anion,[43] it appears that the terminal atoms can be reasonably assigned charges of -0.5 each, while the central carbon is not appreciably charged. The recognition that charge assignment schemes are ultimately arbitrary must be accepted as a limitation in the model. Any scheme designed to circumvent this problem by accounting for the electron distribution in the surrounding lattice necessitates the invocation of quantum mechanical computations.

Another potential source of information about the tensor orientations is the line widths.[23] Intermolecular dipolar interactions contribute to the line widths observed in solid-state NMR experiments. Since the largest component of the dipolar coupling tensor is always along the internuclear vector, a comparison of the relative line widths between sites may permit a qualitative assessment of the orientation sufficient to make assignments. The remote positioning of the cesium atoms in the crystal lattice suggests that such dipole couplings—hetero- and homonuclear—will be small, but they may be large enough to influence the line widths. In the present case, the line width of the central transition does indeed appear to be affected by dipolar interactions and ranges from 180 to 360 Hz for different orientations of the crystal in the applied magnetic field. However, since the variation occurs simultaneously in both sites, this approach is also inconclusive.

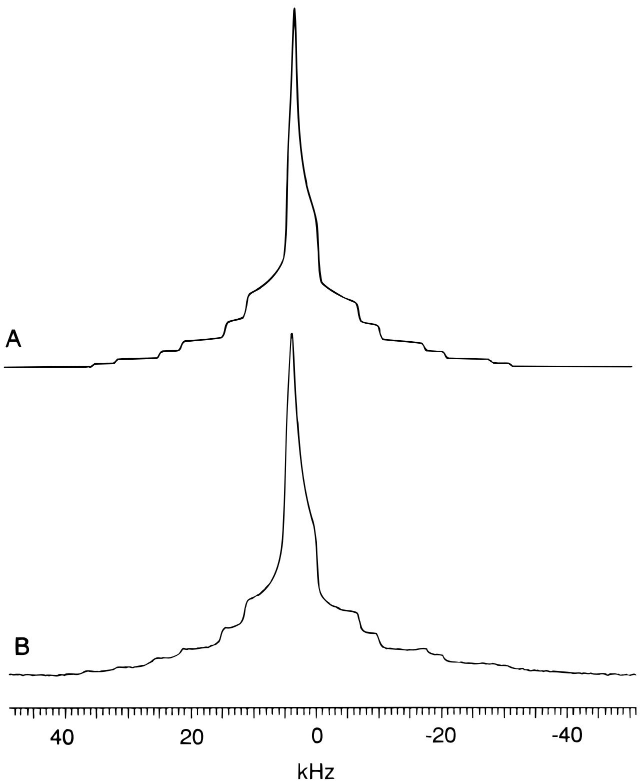

Figure 5. Calculated (A) and experimental (B) cesium-133 NMR powder patterns of $CsCd(SCN)_3$ acquired at 52.48 MHz. Calculated spectrum is based on parameters obtained from single-crystal NMR data: $\delta_{11} = 93.8$ ppm; $\delta_{22} = 72.6$ ppm; $\delta_{33} = -0.6$ ppm; $eQV_{33}/h = 148$ kHz; $\eta_Q = 0.98$; $\alpha = 113°$; $\beta = 105°$; $\gamma = 140°$.

In summary, the orientational assignment of the experimentally determined interaction tensors remains elusive. However, the insight provided by these failed attempts proves valuable: each of the two chemical shielding tensor orientations and each of the electric field gradient orientations appears to be surrounded by similar environments when assigned to the same cesium nucleus, bearing no obvious relation to neighboring nuclei or anionic fragments. The fact that the relative orientations are yet very different emphasises that the orientational behavior of these interaction tensors is exceedingly sensitive to the surrounding environment.

In every example of noncoincidence presented by single-crystal NMR, at least one of the axes is determined by symmetry.[14,15c,20−22] By contrast, the crystal structure of $CsCd(SCN)_3$ indicates that no local symmetry effects are present to impose constraints on the cesium-133 tensors. Correspondingly, the orientations of the chemical shielding and electric field gradient tensors are also free of symmetry constraints. This appears to be the first report of a single-crystal NMR study in which these tensor orientations are completely free of symmetry limitations.

^{133}Cs NMR Spectrum of a Stationary Sample. In order to compare the parameters determined from the single-crystal NMR study, a static spectrum of finely ground $CsCd(SCN)_3$ was obtained at 9.4 T (Figure 5). The calculation of this spectrum required as input the three principal components of the chemical shift tensor, the nuclear quadrupole coupling constant, the asymmetry in the EFG, and three Euler angles to specify the relative orientation of the two tensors. The computed spectrum agrees well with the experiment.

In many cases, when single-crystal NMR data are unavailable, the analysis of static powder patterns can be a challenge. It is

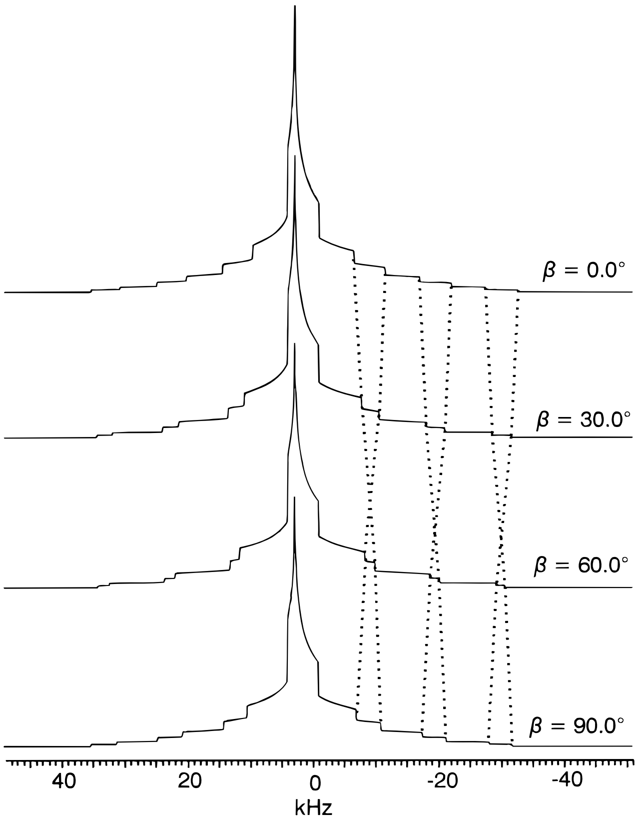

Figure 6. Simulated static cesium-133 NMR spectra depicting variations in the line shape due to systematic modifications of the angle, *β*, between the largest components of the chemical shift and electric field gradient tensors. Dotted lines highlight the movement of the steps. All other parameters as in Figure 5.

instructive to consider how one might proceed in the case of CsCd(SCN)$_3$ without single-crystal data. Assuming negligible second-order quadrupole effects, the central transition can be analyzed to obtain the principal components of the chemical shift tensor. The analysis can become complicated if satellite peak maxima overlap with the shoulders of the central transition, but for CsCd(SCN)$_3$, it appears that these discontinuities are obscured by the span of the chemical shift. Observing no such satellite peak maxima, one surmises that the asymmetry in the electric field gradient is close to 1. If the far outer shoulders are resolved, the total span of the spectrum can be used to compute the magnitude of the quadrupole coupling constant. These five parameters can usually be estimated with relative ease. The remaining challenge is to determine the three Euler angles describing the relative orientation. In the absence of symmetry restrictions, these parameters can be very difficult to identify and will invariably involve extensive “trial and error”.

The importance of knowing the relative tensor orientations in simulations of powder patterns, both spinning and stationary, has been amply evidenced.[26−33] In fact, simulations of first-order quadrupolar patterns can be misleading if incorrect assumptions about the Euler angles are used to simplify the computation. The sensitivity of a static spectrum to a given angle is illustrated by fixing seven parameters in the simulation and varying the angle between the largest components of the two tensors (Figure 6). The positions of the shoulders shift by more than 5 kHz at 9.4 T as the angle, *β*, is increased from 0 to 90°. It is important to note, however, that the sensitivity of the static line shape to a given Euler angle does not necessarily imply that there is a single, well-defined solution in the fitting of a calculated spectrum to the experimental spectrum.

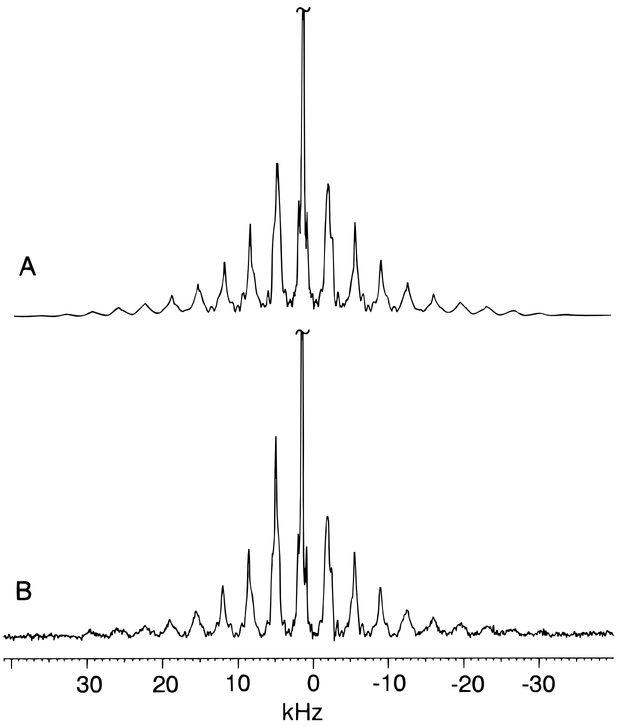

Figure 7. Calculated (A) and experimental (B) cesium-133 VAS spectra of CsCd(SCN)$_3$ acquired in an applied magnetic field of 4.7 T at a spinning angle of 52.25°. The calculated spectrum is based on parameters obtained from single-crystal NMR data (see Figure 5).

There has been a great deal of interest in the development of iterative fitting schemes for powder NMR spectra of quadrupolar nuclei. The motivation is provided, in large part, by the difficulties sometimes encountered in growing sufficiently large single crystal. This limitation often necessitates acquiring NMR spectra of powder samples and attempting to disentangle the respective interactions by simulations of the experimental spectra. However, many pitfalls are associated with this enterprise, and so far, the success of such iterative algorithms has been limited to special cases.

Crucial to the development of any such program are reliable data with which to compare results. Single-crystal NMR is an indispensable tool for this purpose, since results from powder samples must have an independent reference. Therefore, the current study provides a fully characterized model compound for use in testing simulation programs. Moreover, CsCd(SCN)$_3$ provides a rigorous test for iterative fitting methods. Its lack of symmetry for the cesium sites requires that all eight parameters be considered variable. The high asymmetry in the electric field gradient tensor concentrates the satellite peak maxima about the isotropic chemical shift, causing pairs of satellite subspectra to be identical and removing these telltale “horns” from observation.

^{133}Cs NMR Spectra of Spinning Samples. The magic-angle spinning spectrum of CsCd(SCN)$_3$ was acquired in an applied magnetic field of 4.7 T and simulated using the parameters obtained from the single-crystal NMR study. Good agreement is observed between the calculated and experimental spectra.

Variable-angle spinning spectra were also collected at various angles, θ, with respect to the applied magnetic field. The example displayed in Figure 7 shows a spectrum obtained with $\theta = 52.25°$. Agreement between calculated and experimental spectra is good in all cases. The rotation angles were calibrated using VAS ^{133}Cs NMR spectra of cesium thiocyanate in a manner previously described.[44] A static spectrum of finely ground CsSCNacquired at 52.48 MHz exhibited a central transition broadened only by anisotropic chemical shielding and clearly separated from peak maxima associated with the satellites. This central transition powder pattern was analyzed to yield the principal components of the chemical shift tensor in ppm: $\delta_{11} = 139(2)$, $\delta_{22} = 129(2)$, and $\delta_{33} = 30(2)$. Rotation angles calibrated by this technique are estimated to be accurate to within 0.05°. The utility of VAS in the determination of relative tensor orientations is under investigation in our laboratory.

Conclusions

The general usefulness of single-crystal NMR has been demonstrated by the characterization of all relevant ^{133}Cs NMR parameters in $CsCd(SCN)_3$. The chemical shift and electric field gradient tensors are shown to be noncoincident, and the importance of accounting for the relative orientation in simulations of static powder spectra is highlighted. The particularities of this compound underscore the power of single-crystal NMR to resolve multiple interactions and determine absolute tensor orientations irrespective of the atomic positioning, where other techniques may encounter difficulties or fail altogether. As such, this system may serve as a challenge to iterative procedures for simulating powder spectra.

Acknowledgment. We are grateful to the Natural Sciences and Engineering Research Council (NSERC) of Canada for supporting this work through research and equipment grants. Ms. Katherine Robertson is acknowledged for her assistance with some crystallographic aspects of this study. S. K. thanks NSERC, the Walter C. Sumner Foundation, and the Izaak Walton Killam Trust for postgraduate scholarships. R.E.W. is grateful to the Canada Council for a Killam Research Fellowship. All spectra were obtained at the Atlantic Region Magnetic Resonance Centre, supported by NSERC of Canada.

References and Notes

(1) Detellier, C. In *NMR of Newly Accessible Nuclei*; Academic Press: New York, 1983; Vol. 2, pp 105−151.

(2) Dye, J. L.; Ellaboudy, A. S.; Kim, J. In *Modern NMR Techniques and Their Application in Chemistry*; Popov, A. I., Hallenga, K., Eds.; Marcel Dekker: New York, 1991; pp 217−322.

(3) (a) Weiss, C. A., Jr.; Kirkpatrick, R. J.; Altaner, S. P. *Geochim. Cosmochim. Acta* **1990**, *54*, 1655. (b) Weiss, C. A., Jr.; Kirkpatrick, R. J.; Altaner, S. P. *Am. Mineralog.* **1990**, *75*, 970.

(4) Laperche, V.; Lambert, J. F.; Prost, R.; Fripiat, J. J. *J. Phys. Chem.* **1990**, *94*, 8821.

(5) Chu, P. J.; Gerstein, B. C.; Nunan, J.; Klier, K. *J. Phys. Chem.* **1987**, *91*, 3288.

(6) Ahn, M.-K.; Iton, L. E. *J. Phys. Chem.* **1991**, *95*, 4496.

(7) Koller, H.; Burger, B.; Schneider, A. M.; Engelhardt, G.; Weitkamp, J. *Microporous Mater.* **1995**, *5*, 219.

(8) Malek, A.; Ozin, G. A.; MacDonald, P. M. *J. Phys. Chem.* **1996**, *100*, 16662.

(9) Dupree, R.; Kirby, D. J.; Freyland, W. *Z. Naturforsch.* **1982**, *37a*, 15.

(10) (a) Ellaboudy, A.; Dye, J. L.; Smith, P. B. *J. Am. Chem. Soc.* **1983**, *105*, 6490. (b) Dawes, S. B.; Ellaboudy, A. S.; Dye, J. L. *J. Am. Chem. Soc.* **1987**, *109*, 3508. (c) Dawes, S. B.; Eglin, J. L.; Moeggenborg, K. J.; Kim, J.; Dye, J. L. *J. Am. Chem. Soc.* **1991**, *113*, 1605.

(11) (a) Maniwa, Y.; Mizoguchi, K.; Kume, K.; Tanigaki, K.; Ebbesen, T. W.; Saito; Mizuki, J.; Tsai, J. S.; Kubo, Y. *Solid State Commun.* **1992**, *82*, 783. (b) Maniwa, Y.; Mizoguchi, K.; Kume, K.; Kikuchi, K.; Ikemoto, I.; Suzuki, S.; Achiba, Y.; Tanigaki, K.; Ebbesen, T. W.; Saito; Mizuki, J.; Tsai, J. S.; Kubo, Y. *Synth. Mater.* **1993**, *55−57*, 3063.

(12) Tycko, R.; Dabbagh, G.; Murphy, D. W.; Zhu, Q.; Fischer, J. E. *Phys. Rev. B* **1993**, *48*, 9097.

(13) Stenger, V. A.; Pennington, C. H.; Buffinger, D. R.; Ziebarth, R. P. *Phys. Rev. Lett.* **1995**, *74*, 1649.

(14) Gornostansky, S. D.; Stager, C. V. *J. Chem. Phys.* **1967**, *46*, 4959.

(15) (a) Lourens, J. A. J.; Reynhardt, E. C. *Phys. Stat. Sol. A* **1972**, *11*, 739. (b) Lourens, J. A. J.; Reynhardt, E. C. *Phys. Stat. Sol. A* **1972**, *12*, 215. (c) Reynhardt, E. C. *J. Phys. C: Solid State Phys.* **1974**, *7*, 4135.

(16) Baugher, J. F.; Taylor, P. C.; Oja, T.; Bray, P. J. *J. Chem. Phys.* **1969**, *50*, 4914.

(17) Alderman, D. W.; Solum, M. S.; Grant, D. M. *J. Chem. Phys.* **1986**, *84*, 3717.

(18) Ditchfield, R. In *Critical Evaluation of Chemical and Physical Structural Information.* Lide, D. R., Paul, M. A., Eds.; National Academy of Sciences: Washington, DC, 1974; pp 565−590.

(19) Scheubel, W.; Zimmerman, H.; Haeberlen, U. *J. Magn. Reson.* **1985**, *63*, 544.

(20) Boguslavskii, A. A.; Ivanov, Yu. N.; Krieker, A. I.; Mośalev, A. K.; Pakhomov, V. I.; Lotfullin, R. Sh. *Phys. Stat. Sol. B* **1990**, *161*, K49.

(21) Power, W. P.; Mooibroek, S. M.; Wasylishen, R. E.; Cameron T. S. *J. Phys. Chem.* **1994**, *98*, 1552.

(22) Vosegaard, T.; Skibsted, J.; Bildsøe, H.; Jakobsen, H. J. *J. Magn. Reson. A* **1996**, *122*, 111.

(23) (a) Kennedy, M. A.; Ellis, P. D. *Concepts Magn. Reson.* **1989**, *1*, 35. (b) Kennedy, M. A.; Ellis, P. D. *Concepts Magn. Reson.* **1989**, *1*, 109.

(24) Mooibroek, S. Ph.D. Thesis, Dalhousie University, 1987.

(25) Power, W. P.; Wasylishen, R. E. Unpublished results.

(26) Power, W. P.; Wasylishen, R. E.; Mooibroek, S.; Pettitt, B. A.; Danchura, W. *J. Phys. Chem.* **1990**, *94*, 591.

(27) France, P. W. *J. Magn. Reson.* **1991**, *92*, 30.

(28) Amoureux, J. P. *Z. Naturforsch.* **1992**, *47a*, 665.

(29) (a) Cheng, J. T.; Edwards, J. C.; Ellis, P. D. *J. Phys. Chem.* **1990**, *94*, 553. (b) Edwards, J. C.; Zubieta, J.; Shaikh, S. N.; Chen, Q.; Bank, S.; Ellis, P. D. *Inorg. Chem.* **1990**, *29*, 3381. (c) Edwards, J. C.; Adams, R. D.; Ellis, P. D. *J. Am. Chem. Soc.* **1990**, *112*, 8349. (d) Koons, J. M.; Hughes, E.; Cho, H. M.; Ellis, P. D. *J. Magn. Reson. A* **1995**, *114*, 12.

(30) Chung, S. C.; Chan, J. C. C.; Au-Yeung, S. C. F.; Xu, X. *J. Phys. Chem.* **1993**, *97*, 12685.

(31) (a) Hirschinger, J.; Granger, P.; Rosé, J. *J. Phys. Chem.* **1992**, *96*, 4815. (b) Hirschinger, J.; Mongrelet, T.; Marichal, C.; Granger, P.; Savariault, J. M.; Déramond, E.; Galy, J. *J. Phys. Chem.* **1993**, *97*, 10301. (c) Kempgens, P.; Hirschinger, J.; Elbayed, K.; Raya, J.; Granger, P.; Rosé, J. *J. Phys. Chem.* **1996**, *100*, 2045.

(32) (a) Skibsted, J.; Nielsen, N. C.; Bildsøe, H.; Jakobsen, H. J. *Chem. Phys. Lett.* **1992**, *188*, 405. (b) Skibsted, J.; Nielsen, N. C.; Bildsøe, H.; Jakobsen, H. J. *J. Am. Chem. Soc.* **1993**, *115*, 7351. (c) Vosegaard, T.; Skibsted, J.; Bildsøe, H.; Jakobsen, H. J. *J. Phys. Chem.* **1995**, *99*, 10731. (d) Skibsted, J.; Vosegaard, T.; Bildsøe, H.; Jakobsen, H. J. *J. Phys. Chem.* **1996**, *100*, 14872.

(33) (a) Fernandez, C.; Bodart, P.; Amoureux, J. P. *Solid State Nucl. Magn. Reson.* **1994**, *3*, 79. (b) Fernandez, C.; Amoureux, J. P.; Bodart, P.; Maijanen, A. *J. Magn. Reson. A* **1995**, *113*, 205.

(34) Medek, A.; Sachleben, J. R.; Beverwyk, P.; Frydman, L. *J. Chem. Phys.* **1996**, *104*, 5374.

(35) Hayashi, S. *Magn. Reson. Chem.* **1996**, *34*, 791.

(36) Chen, T. H.; Wang, J. Z.; Li, H. K.; Wang, K. X.; Deng, F.; Du, Y. R.; Ding, D. T. *Chem. Phys. Lett.* **1995**, *238*, 82.

(37) Thiele, G.; Messer, D. *Z. Anorg. Allg. Chem.* **1980**, *464*, 255.

(38) Grossmann, H. *Chem. Ber.* **1902**, *35*, 2665.

(39) Volkoff, G. M.; Petch, H. E.; Smellie, D. W. L. *Can. J. Phys.* **1952**, *30*, 270.

(40) Jameson, C. J. In *Nuclear Magnetic Resonance—A Specialist Periodical Report*; Webb, G. A., Ed.; Royal Society of Chemistry: Cambridge, Great Britain, 1996; Vol. 23 and previous volumes in this series.

(41) *Nuclear Magnetic Shieldings and Molecular Structure*; Tossell, J. A., Ed.; NATO ASI Series C.; Kluwer Academic: Dordrecht, The Netherlands, 1993; Vol. 386.

(42) Slichter, C. P. *Principles of Magnetic Resonance*, 3rd ed.; Springer-Verlag: New York, 1990.

(43) Schultz, P. W.; Leroi, G. E.; Harrison, J. F. *Mol. Phys.* **1996**, *88*, 217.

(44) Wu, G.; Wasylishen, R. E. *J. Chem. Phys.* **1994**, *100*, 4828.